14th IEA Heat Pump Conference
15-18 May 2023, Chicago, Illinois

Searching for eco-friendly working fluids for an ejector-driven heat pump for domestic water heating

Ramy H. Mohammed [a], Jeremy Spitzenberger [a], Pengtao Wang [b], Hongbin Ma [a,*], Ahmad Abu-Heiba [c], Stephen Kowalski [b], Kashif Nawaz [b]

[a]Multiphysics Energy Research Center (MERC), College of Engineering, University of Missouri-Columbia, Columbia, MO 65211, USA.
[b]Multifunctional Equipment Integration Group, Building Technologies, Research and Integration Center (BTRIC), Oak Ridge National Laboratory, (ORNL), Oak Ridge, TN 37830.
[c] Rocky Research, Honeywell Aerospace, Boulder City, NV 89005.

Abstract

This study searches for refrigerants with low global warming potential (GWP) and zero ozone depletion potential (ODP) for an ejector heat pump water heater (EHPWH). Several criteria are set, and R1336mzz(Z), R601a, R1233zd(E), R1224yd(Z), R1234ze(Z), and R600a are shortlisted. A theoretical model is built to study the performance of EHPWH and the corresponding ejector design at different operating conditions. For the same ejector design, a refrigerant with a high specific heat ratio produces a high entrainment ratio and heating COP. This is because the expansion wave angle in the ejector is small for refrigerants with a high specific heat ratio, allowing more mass flow rate to be entrained. A higher entrainment ratio does not necessarily correlate to a high COP because the saturation curve of the tested refrigerants is not the same. Results show that the heating COP of R601a is the highest, but it is extremely flammable. R1224yd(Z) and R1234ze(Z) are the most candidates for EHPWH when the trade-off between the COP and safety criteria is considered. The results presented in this work could help building an EHPWH using eco-friendly refrigerants.

Selection and/or peer-review under the responsibility of the organizers of the 14th IEA Heat Pump Conference 2023.

Keywords: Ejector; Heat Pump; Water Heating; COP; Working Fluids; GWP.

Introduction

Buildings are responsible for 40% of global energy consumption and 33% of greenhouse gas emissions. Water heating accounts for about 20% of home's energy use. Using energy efficient water heater can reduce the monthly water heating bills. Ensuring new buildings are sustainable and energy-efficient is key to tackling climate change [1]. The Federal Sustainability Plan has been designed and set goals to reduce energy consumption and achieve net-zero emissions buildings by 2045, including a 50% reduction by 2032 [2]. Heat pump is the widely used technology to produce building cooling and heating energy. The proper working fluid selection for heat pump systems is a key parameter to address the Federal Sustainability Plan's ambitious goals by reducing carbon emissions, greenhouse gases, and energy consumption (i.e., achieving a high coefficient of performance (COP)). The suitable working fluids (refrigerants) should be non-toxicity, non-flammable, non-explosive, and eco-friendly with low Global Warming Potential (GWP) and zero Ozone Depletion Potential (ODP) [3], and have desired thermophysical properties, such as high latent heat of vaporization and high thermal conductivity [4].

The working fluids for cooling and heating systems can be classified into Hydrocarbons (HCs), Chlorofluorocarbons (CFCs), Hydrochlorofluorocarbons (HCFCs), Hydrofluorocarbons (HFCs), Hydrofluoroolefins (HFOs), Hydrofluoroethers (HFEs), Fluorocarbons (FCs), and natural refrigerants. CFCs

* Corresponding author. Tel.: +1 573-884-5944.
E-mail address: mah@missouri.edu.

and HCFCs have high ozone depletion potential (ODP) and were phased out under Montreal Protocol. HFCs with high global warming potential (GWP >150) are being phased out. HCs are A3 flammable refrigerants, and only a few HCs, such as Isobutane (R600a), are approved by US Environmental Protection Agency (EPA) [5]. HFOs are developed as alternative refrigerants with low GWPs to replace HFCs and HCFCs [6]. HFEs are non-flammable fluids with low toxicity, chemically inert, and high-temperature stability. Recently, HFOs and HFEs have been investigated as alternative refrigerants for ejector refrigeration systems [4].

The ejector is a thermal-driven compressor that sucks vapor (secondary fluid) from a vessel at low pressure and lifts to a high pressure using a motive fluid (primary fluid) with higher pressure and temperature. The ejector heat pump for cooling and heating applications consists of an ejector, generator, evaporator, condenser, expansion valve, and pump, as shown in Fig. 1. It has many advantages over the electrically driven heat pump, such as simple construction, no moving parts, high reliability, and low cost, making it attractive for residential systems [7]. The ejector heat pump could be driven by different types of heat sources, such as low-grade waste heat (>70 ℃) and renewable energy [8]. Also, it has good potential to boost primary energy efficiency by avoiding the losses in electric generation and transmissions.

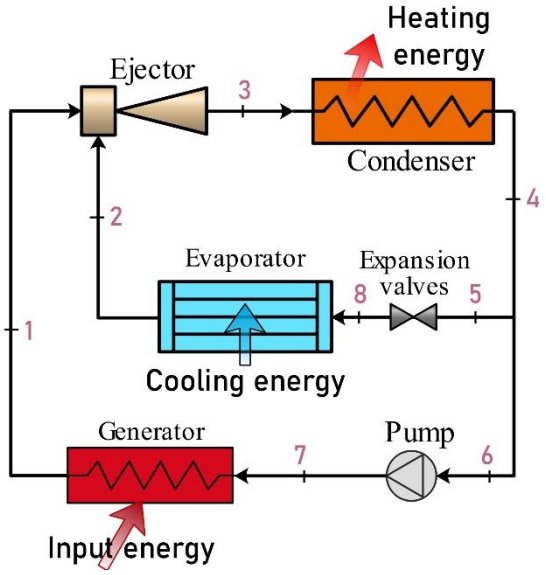

Fig. 1. Schematic drawing of ejector heat pump.

The coefficient of performance (COP) of the ejector heat pump is a function of the entrainment ratio and the ratio between the latent heat of vaporization of secondary fluid and primary fluid. The entrainment ratio is the ratio between the mass flow rate of secondary fluid and primary fluid. It depends on the ejector design, operating conditions, and thermophysical properties of the working fluid. Aphornratana et al. [9] conducted experimental tests for an R11 ejector using two different mixing chambers to study the effect of secondary flow chocking on the ejector performance. The cooling COP of the cycle varied from 0.1 to 0.25. It was found that higher performance is obtained only when the secondary flow is chocked. Ma et al. [10] investigated water and used a spindle to control the water vapor in the primary nozzle according to the heat input. The experimental measurements revealed that a short primary nozzle produces maximum cooling energy, while the longer primary nozzle has a higher COP. Dong et al. [11] reported that the steam ejector cooling cycle could produce a COP of 0.66 when the HTE operates between 55 ºC and 70 ºC. Experimental measurements indicated that the COP decreases when the condenser pressure increases. Shovon et al. [12] tested the performance of a solar refrigeration system's ejector cooling cycle using several working fluids under various operating conditions. The theoretical results highlighted the significant effect of the ejector area ratio on the cycle's COP. Specifically, the COP could be doubled using R718 (water), which increased the ejector area ratio from 6.4 to 12.8, which is defined as the ratio between the constant ejector area and the nozzle throat area. However, the highest COP was calculated using R717 (ammonia), while the maximum cooling effect was produced using water as a working fluid. Geng et al. [13] performed experimental measurements and theoretical analysis to study the performance of the nitrogen ejector cooling cycle. Two primary nozzles with throat diameters of 0.155 mm and 0.185 mm were investigated. Test results showed that the back pressure rises when higher inlet temperatures for the evaporator and generator are used.

Previous studies revealed that the performance ejector cycle depends on the operating conditions and

design parameters. Also, the ejector should be designed for a specific working fluid to achieve higher performance. It is found that little attention has been paid to the ejector cycle for heating applications. Hence, there is a lack of identifying a proper eco-friendly working fluid and corresponding ejector design. Therefore, this study screens different working fluids for ejector heat pump for water heating (EHPWH) that uses a working fluid with low GWP and zero ODP, while the cycle operates under positive pressure with a high heating COP. Criteria for working fluid pairs are established, and candidates for EHPWH are shortlisted. A thermodynamic model for EHPWH is built to evaluate its heating COP using the shortlisted working fluids at various operating parameters. The corresponding geometrical specifications of the ejector are presented.

2. Criteria for selecting the working fluid pairs

The criteria for working fluids screening are established based on having low GWP and zero ODP. Table 1 lists the selected working fluids for GHPWH. In the EHPWH, the evaporator operates at the ambient temperature of 19.4 ℃ as specified for rating air-source heat pump water heaters by the US Department of Energy [33]. It assumed that the evaporator pinch point is 5.0 ℃. Therefore, the evaporation temperature is set at 14.4 ℃. Based on this temperature, the saturation pressure is estimated to identify which working fluid makes the system operates under a vacuum.

The Mach number at the exit of the primary nozzle affects the back pressure. This Mach number is a function of the working fluid's molecular weight and specific heat ratio. R1234ze(Z), R1234ze(E), and R1234yf have the same molecular weight. So, R1234ze(Z) is selected for investigation because its critical temperature is the highest, allowing the generator of heat pump to work at high temperature and subcritical conditions, and hence achieve higher condenser temperature for the same ejector design. R290 and R1270 have relatively low critical temperatures (less than 100 ℃), making them unsuitable for heat pump water heater that could produce hot water at 50 ℃. R717 is usually a suitable refrigerant for chillers, not for heat pumps. Therefore, R601a, R1336mzz(Z), R1233zd(E), R1224yd(Z), R1234ze(Z), and R600a are investigated in this study.

Table 1. Selected refrigerants with low GWP and zero ODP for EHPWH.

	Refrigerants	Chemical Name	P_{sat}* [bar]	T_{cr} [℃]	P_{cr} [bar]	NBP [℃]	γ	MW [kg/kmol]	ODP	GWP (AR4**)	SC+
Under vacuum	R1336mzz(Z)	cis-1,1,1,4,4,4-Hexafluoro-2-butene	0.475	171.3	29	33.5	1.074	164.1	0	2	A1
	R601a	Isopentane	0.620	187.2	33.7	27.9	1.092	72.15	0	4	A3
	R1233zd(E)	Trans-1-chloro-3, 3, 3-Trifluoropropene	0.871	165.6	35.73	18.3	1.105	130.5	0	1	A1
	R1224yd(Z)	cis-1-chloro-2,3,3,3-tetrafluoropropene	0.98	155.5	33.37	14.6	1.104	148.5	0	< 1	A1
Above atmospheric	R1234ze(Z)	cis-1, 3, 3, 3-Tetrafluoropropene	1.21	150.1	35.31	9.7	1.133	114	0	7	A2L
	R600a	Isobutane	2.54	134.7	36.4	-11.7	1.139	58.12	0	< 5	A3
	R1234ze(E)	Trans-1,3,3,3-tetrafluoro-1-propene	3.59	109.4	36.32	-19.3	1.15	114	0	7	A2L
	R1234yf	2,3,3,3-tetrafluoro-1-propene	5.01	94.7	33.82	-29.5	1.177	114	0	< 5	A2L
	R717	Ammonia	7.14	132.3	113.3	-33.3	1.435	17.03	0	0	B2
	R290	Propane	7.20	96.68	42.47	-42.1	1.251	44.1	0	< 5	A3
	R1270	Propylene	8.80	92.42	46.65	-47.7	1.303	42.08	0	2	A3

* Pressure calculated at T = 14.4 ºC.
** AR4 refers to the Intergovernmental Panel on Climate Change (IPCC) Fourth Assessment Report (2007) https://www.ipcc.ch/report/ar4/syr/
+ASHRAE safety class (SC): A and B for toxicity from low to high, 1, 2L, 2, and 3 for flammability from low to high.

3. Theoretical Model

A one-dimensional model is implemented in this study based on the following assumptions [14,15]:

1) The working fluids in the ejector are ideal gas with constant thermodynamic properties.
2) The process of the ejector is a steady state.
3) The flow inside the ejector is one-dimensional.
4) Inlet and outlet kinetic energies are neglected.
5) The irreversibility is respected using experimental coefficients, except that isentropic processes are considered.
6) The ejector walls are adiabatic.
7) Mixing primary (pf) and secondary (sf) streams starts at y–y (refer to Fig. 2).
8) Normal shockwave occurs after mixing primary and secondary streams (at section s-s).

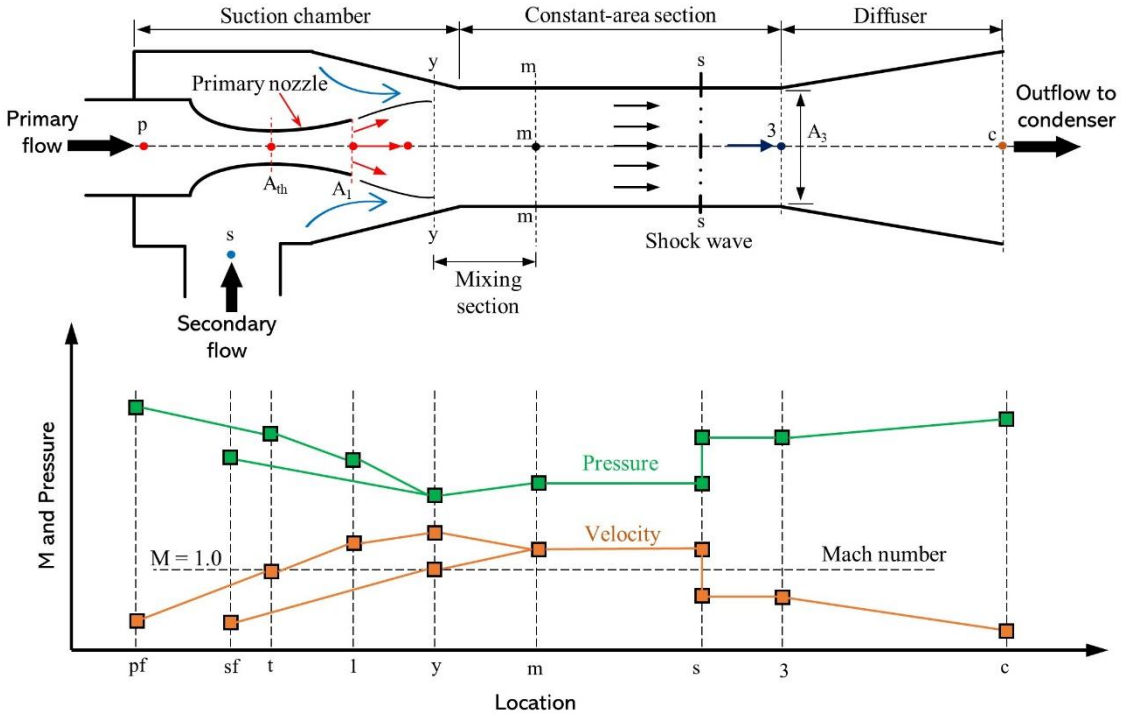

Fig. 2. (a) A detailed schematic of the used ejector and (b) pressure and Mach number variation along the ejector (adapted from [14,16]).

The primary mass flow rate (coming from the generator) can be expressed as a function of temperature, pressure, and throat area.

$$\dot{m}_{pf} = \frac{P_g A_{th}}{\sqrt{T_g}} \sqrt{\frac{\gamma}{R}\left(\frac{2}{\gamma+1}\right)^{\frac{\gamma+1}{\gamma-1}}} \sqrt{\eta_{pn}} \tag{1}$$

where the primary nozzle isentropic efficiency (η_{pn}) is taken as 0.85.

$$\frac{A_1}{A_t} \approx \frac{1}{M_{p1}}\left[\frac{2}{\gamma+1}\left(1+\frac{\gamma-1}{2}M_{p1}^2\right)\right]^{\frac{\gamma+1}{2(\gamma-1)}} \tag{2}$$

$$\frac{P_g}{P_{p1}} \approx \left(1+\frac{\gamma-1}{2}M_{p1}^2\right)^{\frac{\gamma}{\gamma-1}} \tag{3}$$

At y-y location, both streams (p and s) have the same pressure ($P_{py} = P_{sy}$). If it is assumed that the entrained flow is sonic at this location, the pressure ratio can be written as:

$$\frac{P_e}{P_{sy}} \approx \left(\frac{\gamma+1}{2}\right)^{\frac{\gamma}{\gamma-1}} \tag{4}$$

$$\frac{P_{py}}{P_{p1}} \approx \left(\frac{1 + \frac{\gamma - 1}{2} M_{p1}^2}{1 + \frac{\gamma - 1}{2} M_{py}^2} \right)^{\frac{\gamma}{\gamma - 1}} \tag{5}$$

A coefficient ϕ_p is added to the isentropic relation to account for viscous losses at the boundary between both streams. ($\phi_p = 0.95$). The area ratio of the expansion wave can be estimated from the following Equation:

$$\frac{A_{py}}{A_1} = \frac{\phi_p M_{p1}}{M_{py}} \left[\frac{1 + \frac{\gamma - 1}{2} M_{py}^2}{1 + \frac{\gamma - 1}{2} M_{p1}^2} \right]^{\frac{\gamma + 1}{2(\gamma - 1)}} \tag{6}$$

The secondary (coming from the evaporator) mass flow rate is estimated by,

$$\dot{m}_{sf} = \frac{P_e A_{sy}}{\sqrt{T_e}} \sqrt{\frac{\gamma}{R} \left(\frac{2}{\gamma + 1} \right)^{\frac{\gamma + 1}{\gamma - 1}}} \sqrt{\eta_{sn}} \tag{7}$$

Here, the isentropic efficiency of flow expansion (ηsn) is assumed to be 0.85. The total cross-section area at y-y is the same as that of the duct that extends to the aftershock region,

$$A_3 = A_{py} + A_{sy} \quad and \quad AR = \frac{A_3}{A_t} \tag{8}$$

where AR is the ejector area ratio.

Gas dynamic relations are used to specify the temperatures of streams based on upstream Mach number as,

$$\frac{T_g}{T_{py}} = 1 + \frac{\gamma - 1}{2} M_{py}^2 \tag{9}$$

$$\frac{T_e}{T_{sy}} = 1 + \frac{\gamma - 1}{2} M_{sy}^2 \tag{10}$$

A section m-m, both streams are assumed to be totally mixed. Thus, a mixing loss coefficient, ϕ_m, is introduced in the momentum equation between sections m-m and y-y as,

$$\phi_m \left(\dot{m}_p u_{py} + \dot{m}_s u_{sy} \right) = \left(\dot{m}_p + \dot{m}_s \right) u_m \tag{11}$$

Besides, the energy equation is written as,

$$\dot{m}_{pf} \left(h_{py} + \frac{u_{py}^2}{2} \right) + \dot{m}_{sf} \left(h_{sy} + \frac{u_{sy}^2}{2} \right) = \left(\dot{m}_{pf} + \dot{m}_{sf} \right) \left(h_m + \frac{u_m^2}{2} \right) \tag{12}$$

The velocities at different sections can be estimated using Mach number as,

$$\boldsymbol{u_{py} = M_{py} \sqrt{\gamma_{pf} R T_{py}}} \tag{13}$$

$$\boldsymbol{u_{sy} = M_{sy} \sqrt{\gamma_{sf} R_{sf} T_{sy}}} \tag{14}$$

$$\boldsymbol{u_m = M_m \sqrt{\gamma_m R_m T_m}} \tag{15}$$

After the two fluids completely mix, the flow is subjected to a normal shock at section s-s, resulting in an increase in the flow pressure from $P_m = P_{sy} = P_{py}$ to P_3. Then, the state '3' is connecting with state 'c'

(condenser pressure) through a diffusing process.

$$\frac{P_3}{P_m} = 1 + \frac{2\gamma}{\gamma + 1}(M_m^2 - 1) \tag{16}$$

$$M_3^2 = \frac{1 + \frac{\gamma - 1}{2} M_m^2}{\gamma M_m^2 - \frac{\gamma - 1}{2}} \tag{17}$$

$$\frac{P_c}{P_3} = \left(1 + \frac{\gamma - 1}{2} M_3^2\right)^{\frac{\gamma}{\gamma - 1}} \tag{18}$$

After finding the entrainment ratio, the COP of heat pump can be estimated as given:

$$COP = 1 + \frac{\dot{m}_{sf}}{\dot{m}_{pf}} \times \frac{(h_v|_{T_e} - h_l|_{T_c})}{(h_v|_{T_g} - h_l|_{T_c})} = 1 + ER \times \frac{(h_v|_{T_e} - h_f\big|_{T_c})}{(h_v|_{T_g} - h_f\big|_{T_c})} \tag{19}$$

where ER is the ejector entrainment ratio, h_v is the specific enthalpy of saturated vapor, and h_f is the specific enthalpy of saturated liquid.

4. Model validation

The thermodynamic model is built in Engineering Equation Solver (EES) software. The results obtained from the present model are compared with previous experimental data from the literature. Table 2 presents a comparison between the present results and previous ones under the same operating conditions. It is found that the relative error is always less than 4%, indicating that the model is suitable for investigating the performance of ejector cycle.

Table 2. Comparison between present results and previous experimental data for ejector heat pump.

T_g (°C)	Previous results [15]	Present model	Error (%)
120	0.6849	0.6615	3.42
125	0.6074	0.5864	3.45
130	0.5299	0.5158	2.66
135	0.4544	0.4671	2.79
140	0.3822	0.3920	2.56

5. Results and Discussion

This section discusses the effect of the generator pressure and condenser temperature on the ejector area ratio (AR), the entrainment ratio (ER), and COP using the shortlisted working fluids. Discussion is presented about how the thermodynamic properties of the investigated refrigerants affect the ejector behavior and hence the COP of EHPWH.

5.1. Effect of working fluid

For a specific ejector design with an area ratio of 30, the entrainment ratio, mixing Mach number, and corresponding condenser temperature are presented in Fig. 3 for the investigated refrigerants. According to Equation (6), the expansion wave's angle increases when the working fluid's specific heat ratio decreases. This means that the surface area from which the secondary flow is entrained (A_{sy}) decreases when the specific heat ratio of the working fluid decreases. This leads to a decrease in the secondary flow mass flow rate and hence a reduction in the ejector entrainment ratio. So, it is found that the entrainment ratio is the highest using R600a because it has the highest specific heat ratio among the investigated refrigerants (see Table 1). The entrainment ratio of the ejector using R600a is about 3.27 at a heating COP of 3.42. However, R600a produces the lowest value of condenser temperature because the Mach number in the mixing section is found to be the lowest one. On the other hand, R1336mzz(Z) produces the highest condenser temperature of about 50 °C, which is more suitable for heating purposes. However, the entrainment ratio is the lowest and equals 0.4. Thus, for the same ejector, the trend of condenser temperature is always opposite to the trend of the entrainment ratio.

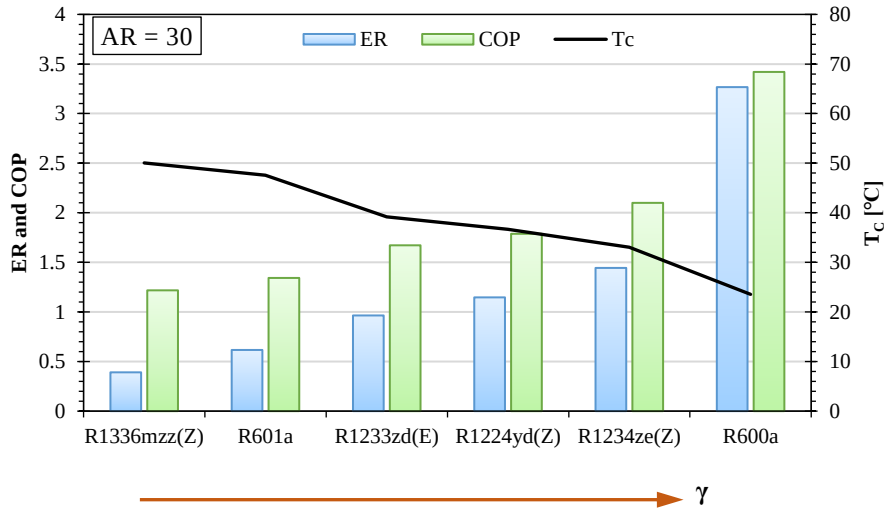

Fig. 3. ER and condenser pressure of ejector heat pump using different refrigerants at constant ejector area ratio at P_g = 25 bar.

Fig. 4 presents the entrainment ratio, Mach number in the mixing chamber, and ejector area ratio using the investigated working fluids to achieve a condenser temperature of 50 °C. All the investigated working fluids achieve almost similar COP of around 1.22 using different ejector area ratios. R601a achieves the highest entrainment ratio of about 0.51 and the highest heating COP of 1.28 using an ejector with an area ratio of 26.5. This behavior is because the generator temperature is the highest for R601a, which is about 168 °C. The ejector area ratio is the largest when the system uses R1336mzz(Z) due to its largest molecular weight of 164.1 kg/kmol. R600a could produce the required condenser temperature of 50 °C using the smallest ejector design of an area ratio of about 6.0 because R600a has the lowest molecular weight (see

Table 1). The entrainment ratio and COP of R1233zd(E), R1224yd(Z), and R1234ze(z) are comparable, but R1224yd(Z) needs a bigger ejector to be able to achieve the desired condenser temperature.

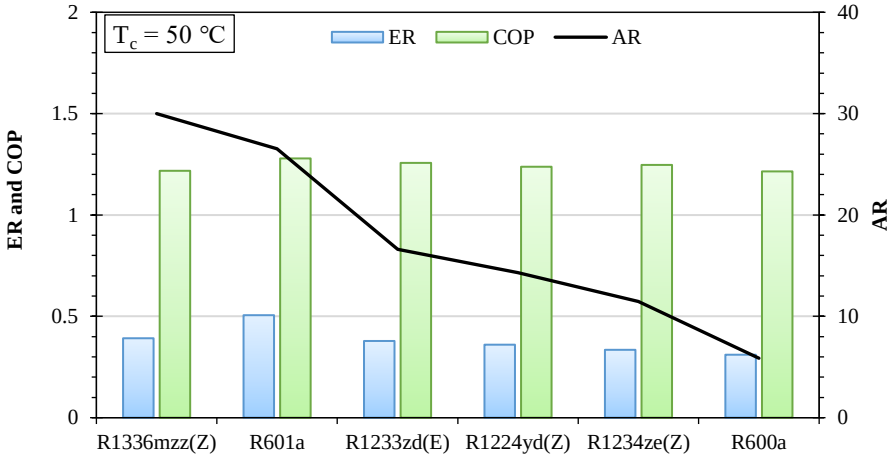

Fig. 4. ER and ejector area ratio of ejector heat pump using different refrigerants at constant condenser pressure at P_g = 25 bar.

5.2. Effect of generator pressure

Fig. 5 presents the variation of ER at various generator pressures for the investigated working fluids. It is found that the ER increases as the generator pressure increases to achieve the same condenser temperature. It can be highlighted that the ER mainly depends on the generator temperature when the generator pressure is fixed. The ER of the ejector using R601a is always the highest and changes from 0.22 to 0.56 when the generator pressure changes from 1000 kPa to 3000 kPa, respectively. The highest ER of R601a is owing to the highest generator temperature. In turn, at any generator pressure, the generator temperature is the lowest when R600a is used, leading to the lowest value of ER.

The area ratio does not follow the same trend, as shown in Fig. 6. To achieve the same condenser pressure, the ejector area ratio should be high for working fluid with large molecular weight. Because R1233mzz(Z) has the highest value of the molecular weight, the ejector area ratio is the highest. For the heating COP, its trends do not follow the trends of ER, as presented in Fig. 7. R601a achieves the highest COP due to its highest ER. Interestingly, the heating COP of EHPWH using R1234ze(Z) rapidly increases and approaches the COP of R601a when the generator pressure increases. This behavior is due to the shape of the saturation curve (P-h diagram) of R1234ze(Z), where the latent heat of vaporization significantly decreases as the pressure increases, and hence the heat added in the generator decreases, leading to a remarkable increase in the heating COP. When the generator pressure changes from 1000 kPa to 3000 kPa, the heating COP produced using R601a and R1234ze(Z) increases by 15% and 26%, respectively. It is worth mentioning that the highest ER does not always correspond to the highest COP of EHPWH. The shape of the P-h diagram of refrigerant affects the amount of heat added in the generator and evaporator and hence the COP accordingly.

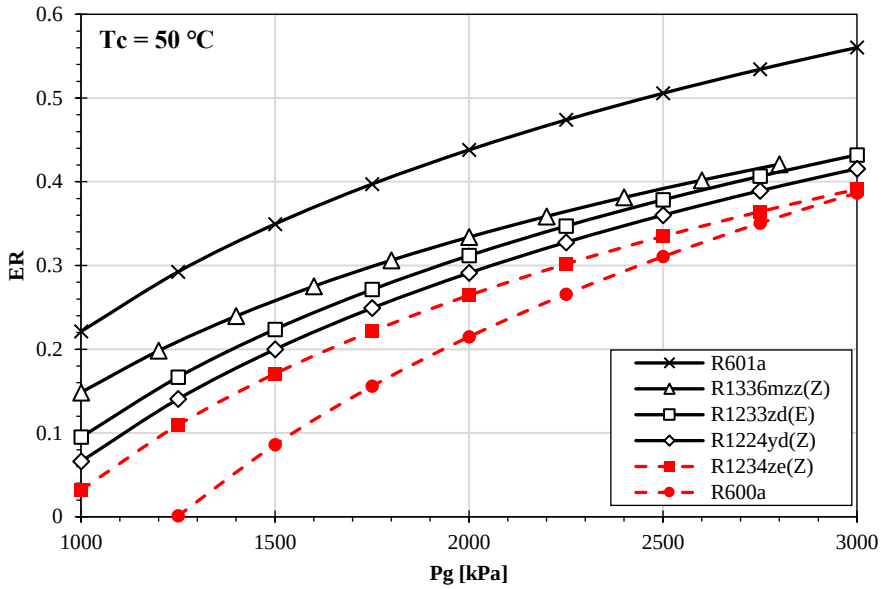

Fig. 5. Effect of generator pressure on the ER at a condenser temperature of 50 °C. (Solid lines indicate operation under vacuum and Dashed lines indicate operation above atmospheric).

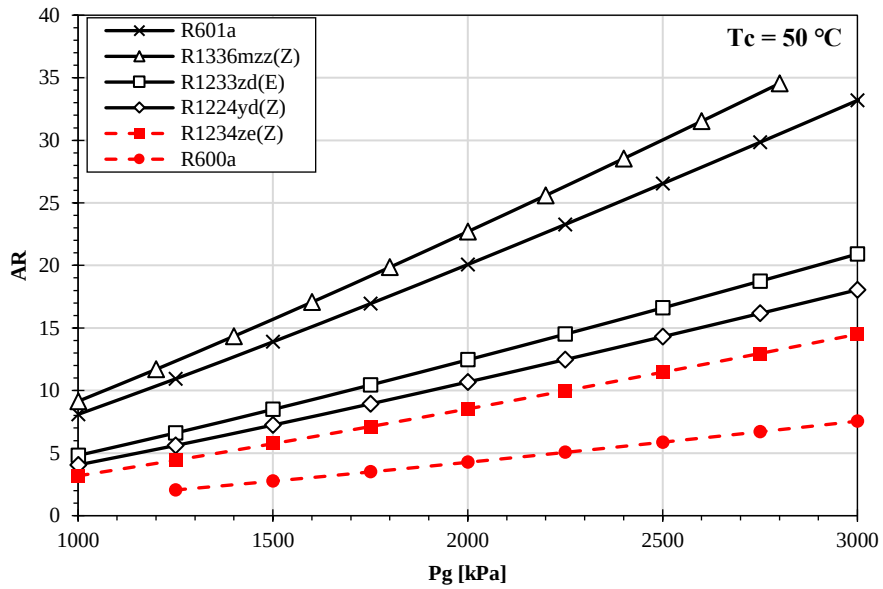

Fig. 6 Effect of generator pressure on the AR at a condenser temperature of 50 °C. (Solid lines indicate operation under vacuum and Dashed lines indicate operation above atmospheric).

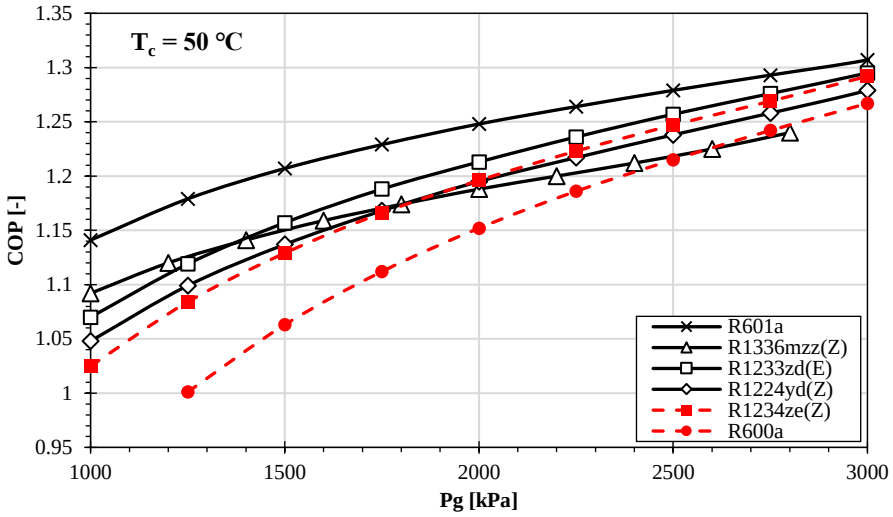

Fig. 7 Effect of generator pressure on the COP at a condenser temperature of 50 °C. (Solid lines indicate operation under vacuum and Dashed lines indicate operation above atmospheric).

5.3. Effect of condenser temperature

The variations of ER for the investigated refrigerants at various condenser temperatures are plotted in Fig. 8. It is found that the ER declines exponentially when the condenser temperature increases for the same ejector design of an area ratio of 30. Regardless of the condenser temperature, the ER is always the highest for R601a, followed by R1336mzz(Z). For R601a, the ER declines from 3.7 to 0.5 (more than 7 times reduction) when the condenser temperature changes 25 °C 50 °C, respectively. This remarkable reduction is observed for all investigated refrigerants. This means that the ejector is very sensitive to condenser pressure, and it should be designed to a specific condenser temperature to be able to achieve higher ER. For Fig. 9, a refrigerant with a larger molecular weight needs a bigger ejector to be able to achieve the desired condenser temperature. Regardless of the variation in ER and AR, the heating COP of EHPWH barely changes when the type of the investigated refrigerant changes, as plotted in Fig. 10. R1234ze(Z) produces the highest COP when the condenser temperature is 25 °C. When the condenser temperature is 25 °C, the heating COP varies between 3.1 and 3.4 when different refrigerants are tested. When the condenser temperature is 40 °C, the heating COP is about 1.22 for the studied refrigerants. Therefore, when the safety class and working around atmospheric pressure or higher, it can be concluded that R1224yd(Z) and R1234ze(Z) are the most suitable candidates for EHPWH to produce hot water at about 50 °C.

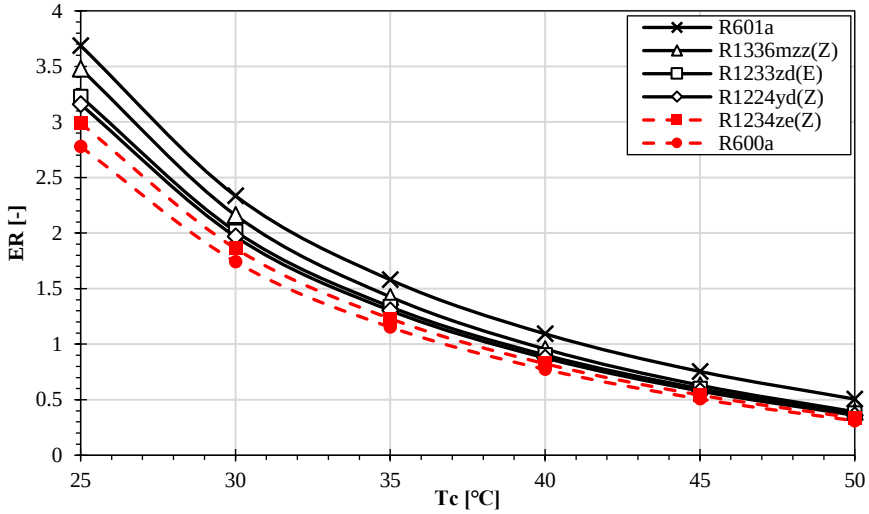

Fig. 8 Effect of condenser temperature on the ER at a generator pressure of 25 bar. (Solid lines indicate operation under vacuum and Dashed lines indicate operation above atmospheric).

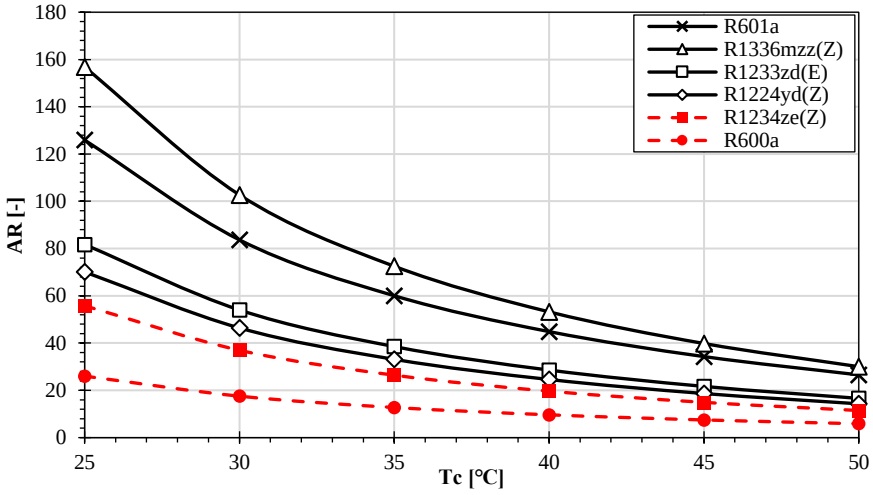

Fig. 9. Effect of condenser temperature on the AR at a generator pressure of 25 bar. (Solid lines indicate operation under vacuum and Dashed lines indicate operation above atmospheric).

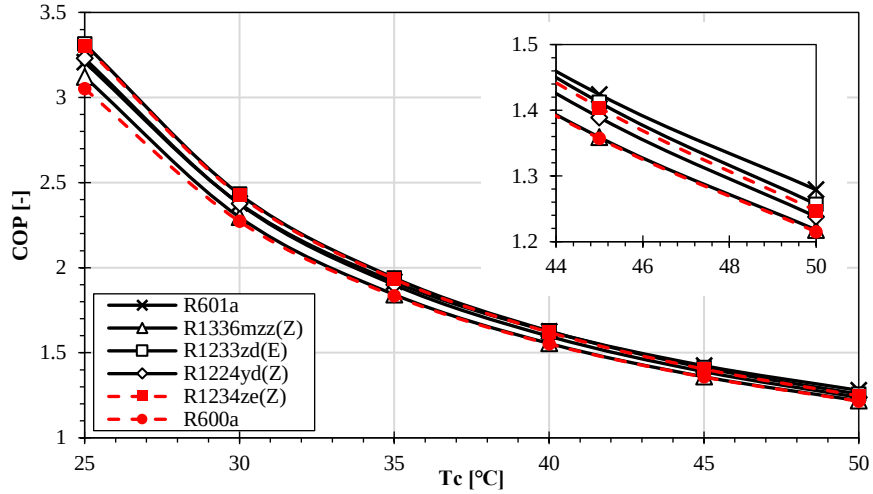

Fig. 10. Effect of condenser temperature on the COP at a generator pressure of 25 bar. (Solid lines indicate operation under vacuum and Dashed lines indicate operation above atmospheric).

6. Conclusion

The present study screens the available working fluids to identify the most suitable environmentally friendly refrigerants for EHPWH. A certain number of refrigerants with low GWP and zero ODP is shortlisted. A mathematical model is built to study the performance of EHPWH using the shortlisted refrigerants at different operating parameters. It is found that refrigerant with large molecular weight always needs a big ejector to achieve desired condenser temperature. It is highlighted that the heating COP is very sensitive to the condenser temperature. Thus, the ejector should be designed for specific operating conditions to be able to achieve high performance. Results indicate that the high ER does not always guarantee the high COP of EHPWH due to the change in the P-h diagram of the tested refrigerants. R601a and R1233zd(E) achieve the highest COP at any condenser temperature, while all the tested refrigerants produce similar heating COP at a condenser temperature of 50 °C. It can be concluded that R1224yd(Z) and R1234ze(Z) are suitable candidates for EHPWH when the trade-off between the COP, toxicity, flammability, and avoiding operating under low vacuum is considered.

Acknowledgments

This material is based upon work supported by the U.S. Department of Energy, Office of Science, Building Technologies Office. This research used resources of the Building Technologies Research and Integration Center (BTRIC) of the Oak Ridge National Laboratory, which is a DOE Office of Science User Facility.

References

[1] Buildings are the foundation of our energy-efficient future | World Economic Forum n.d. https://www.weforum.org/agenda/2021/02/why-the-buildings-of-the-future-are-key-to-an-efficient-energy-ecosystem/ (accessed November 6, 2022).

[2] Federal Sustainability Plan: Catalyzing America's Clean Energy Industries and Jobs | Office of the Federal Chief Sustainability Officer n.d. https://www.sustainability.gov/federalsustainabilityplan/ (accessed October 4, 2022).

[3] Shen B, Nawaz K, Elatar A. Parametric studies of heat pump water heater using low GWP refrigerants. International Journal of Refrigeration 2021;131:407–15. https://doi.org/10.1016/J.IJREFRIG.2021.07.015.

[4] Gil B, Kasperski J. Efficiency analysis of alternative refrigerants for ejector cooling cycles. Energy Convers Manag 2015;94:12–8. https://doi.org/10.1016/j.enconman.2015.01.056.

[5] Chen Q, Yu M, Yan G, Yu J. Thermodynamic analyses of a modified ejector enhanced dual temperature refrigeration cycle for domestic refrigerator/freezer application. Energy 2022;244:122565. https://doi.org/10.1016/J.ENERGY.2021.122565.

[6] Refrigerants With Low Global Warming Potential n.d. https://facilityexecutive.com/2017/02/refrigerants-low-global-warming-potential/ (accessed November 6, 2022).

[7] Tashtoush BM, Al-Nimr MA, Khasawneh MA. A comprehensive review of ejector design, performance, and applications. Appl Energy 2019;240:138–72. https://doi.org/10.1016/J.APENERGY.2019.01.185.

[8] Dong J, Chen X, Wang W, Kang C, Ma H. An experimental investigation of steam ejector refrigeration system powered by extra low temperature heat source. International Communications in Heat and Mass Transfer 2017;81:250–6. https://doi.org/10.1016/J.ICHEATMASSTRANSFER.2016.12.022.

[9] Aphornratana S, Chungpaibulpatana S, Srikhirin P. Experimental investigation of an ejector refrigerator: Effect of mixing chamber geometry on system performance. Int J Energy Res 2001;25:397–411. https://doi.org/10.1002/ER.689.

[10] Ma X, Zhang W, Omer SA, Riffat SB. Performance testing of a novel ejector refrigerator for various controlled conditions. Int J Energy Res 2011;35:1229–35. https://doi.org/10.1002/ER.1766.

[11] Dong J, Hu Q, Xia Y, Song H, Ma H, Cui W, et al. Experimental investigation of a miniature ejector using water as working fluid. J Therm Sci Eng Appl 2020;12. https://doi.org/10.1115/1.4047553.

[12] Shovon MKB, Raman SK, Suryan A, Kim TH, Kim HD. Performance of ejector refrigeration cycle based on solar energy working with various refrigerants. J Therm Anal Calorim 2020;141:301–12. https://doi.org/10.1007/s10973-020-09319-1.

[13] Geng L, Cao H, Meng Q, Li J, Jiang P. Effects of operating conditions and geometries on the performance of nitrogen ejectors for Joule–Thomson cooling. Appl Therm Eng 2022;212:118557. https://doi.org/10.1016/J.APPLTHERMALENG.2022.118557.

[14] Huang BJ, Chang JM, Wang CP, Petrenko VA. A 1-D analysis of ejector performance. International Journal of Refrigeration 1999;22:354–64. https://doi.org/https://doi.org/10.1016/S0140-7007(99)00004-3.

[15] Eames IW, Aphornratana S, Haider H. A theoretical and experimental study of a small-scale steam jet refrigerator. International Journal of Refrigeration 1995;18:378–86. https://doi.org/10.1016/0140-7007(95)98160-M.

[16] Shovon MKB, Raman SK, Suryan A, Kim TH, Kim HD. Performance of ejector refrigeration cycle based on solar energy working with various refrigerants. J Therm Anal Calorim 2020. https://doi.org/10.1007/s10973-020-09319-1.